Electronic Supplementary Material (ESI) for Physical Chemistry Chemical Physics

Charge transport in poly-imidazole membranes: a fresh appraisal of the Grotthuss mechanism

Giuseppe Felice Mangiatordi, Valeria Butera, Nino Russo, Damien Laage and Carlo Adamo

SUPPLEMENTARY INFORMATION

Contents

1. Force field parameterization

The General Amber Force Field (GAFF) assigns a type to each atom according to its orbital hybridization and bonding connectivity.[S1-S2] The atom numbers, the atom types and the relatives RESP[S3-S4] partial charges computed for the protonated imidazole trimer (*3mer*$^+$) and protonated oligomer (*15mer*+) are listed in tables S1 and S2. All the intramolecular interaction parameters published by Voth and coworkers[S5] for imidazole and imidazolium have been included in the parameterized force field. An exception is represented by the two equilibrium angular bending parameters, which have been replaced by the DFT values, significantly different (see Table S3). Furthermore, a value of force constant relative to the dihedrals describing the torsion around the CC bond connecting the central imidazolium to the polymer backbone not presented in the original force field has been included. In particular a k_d = 5.5 kcal/mol has been selected in order to reproduce the DFT data for the corresponding torsional energy for the *3mer*$^+$.
The rotational barrier is in perfect agreement with the DFT data (10.6 kcal/mol vs. 10.7 kcal/mol) and the energy profile obtained has a close shape of that calculated at DFT level (see figure S1).

2. Umbrella sampling technique and weighted histogram analysis method (WHAM)

In all umbrella sampling calculations[S6] carried out for the calculation of the free energy profiles reported in figure 8, dynamics have been run for 2 ns and a force constant for the harmonic bias potential of k = 120 kcal/mol/rad^2 has been used. Windows of 10 degrees have been considered along the reaction coordinates represented by a torsion angle of the investigated system. To determinate the potentials of mean force (PMF) the results have been processed using the weighted histogram analysis method (WHAM).[S7, S8] The bin dimension applied in the WHAM equation has been equal to 2 degrees.

3.Details on MD simulation on 15mer$^+$

The molecular dynamics simulation has been performed keeping fix the carbons of the backbone to the optimized B3LYP/6-31G(d) structure, so to simulate an locally linear rearrangement as in the real system and minimize spurious model effects arising from the consideration of a single polymer chain, such as coiling during MD simulations.

4. Comment on the use of Force Field for the studied mechanism

The frustrated rotation, the key step in the proposed mechanism, involves the breaking and formation of H-bond. This process could be not correctly reproduced by a force field using fixed

charges. In order to verified this point, the atomic charges for the atoms involved in the formation of the hydrogen bond, namely N_3a,H_3b and N3b, are reported in table S4, while the computed electrostatic potential is reported in figure S3. As can be seen from the values collected in table S4, charge computed with the NBO model[S9] do not change along the rotation, while small variations are observed for the RESP charges, which, however, decrease of only 10%. No significant variation can be detected for the electrostatic potential (see figure S3). These results further support the quality of the MD simulations

References

S1 J. Wang, R. M. Wolf, J. W. Caldwell, P. A. Kollman and D. A. Case, *J. Comput. Chem.,* 2004, **25**, 1157-1174.

S2 J. Wang, W. Wang, P. A. Kollman and D. A. Case, *J. Mol. Graph. Model.,* 2006, **25**, 247-260.

S3 C. I. Bayly, P. Cieplak, W. D. Cornell and P. A. Kollman, *J. Phys.Chem.,* 1993, **97**, 10269-10280.

S4 W. D. Cornell, P. Cieplak, C. I. Bayly and P. A. Kollman, *J. Am.Chem. Soc.,* 1993, **115**, 9620-9631.

S5 H. Chen, T. Yan and G. A. Voth, *J. Phys. Chem A,* 2009, **113**, 4507– 4517.

S6 G. M. Torrie and J. P. Valleau, *Chem. Phys. Lett.,* 1974, **28**, 578–581.

S7 S. Kumar, D. Bouzida, R. H. Swendsen, P. A. Kollman and J. M. Rosenberg, *J. Comput. Chem.,* 1992, **13**, 1011-1021.

S8 S. Kumar, J. M. Rosenberg, D. Bouzida, R. H. Swendsen and P. A. Kollman, *J. Comput. Chem.,* 1995, **16**, 1339-1350.

S9 A. E. Reed, L. A. Curtiss and F. Weinhold, *Chem. Rev.*, 1988, **88**, 899.

Table S1. Atom numbers, GAFF atom types and relative RESP partial charges obtained for *3mer*$^{+}$.

atom number	GAFF atom type	q (e)
1	c3	-0.156
2	hc	0.077
3	hc	0.077
4	c3	-0.005
5	hc	0.052
6	c3	-0.156
7	hc	0.077
8	hc	0.077
9	c3	0.070
10	hc	0.040
11	c2	-0.101
12	c2	-0.035
13	h4	0.167
14	h5	0.248
15	cd	-0.201
16	h4	0.196
17	cd	0.164
18	h5	0.143
19	c2	0.076
20	cc	0.155
21	na	-0.108
22	na	-0.209
23	nc	-0.468
24	na	-0.318
25	hn	0.363
26	c3	-0.105
27	hc	0.032
28	hc	0.032
29	hc	0.032
30	hn	0.381
31	c3	0.070
32	hc	0.040
33	c3	-0.105
34	hc	0.032
35	hc	0.032
36	hc	0.032
37	cd	-0.201
38	cd	0.164
39	h4	0.196
40	h5	0.143
41	cc	0.155
42	na	-0.318
43	nc	-0.468
44	hn	0.272
45	hn	0.363

Table S2. Atom numbers, GAFF atom types and relative RESP partial charges obtained for *15mer*$^{+}$.

atom number	GAFF atom type	q (e)
1	c3	0.186
2	c3	-0.379
3	hc	0.099
4	hc	0.099
5	c3	0.104
6	hc	0.067
7	c3	-0.007
8	hc	0.014
9	hc	0.014
10	c3	0.021
11	c3	-0.353
12	hc	0.074
13	hc	0.074
14	c3	-0.036
15	hc	0.106
16	c3	0.035
17	hc	0.043
18	hc	0.043
19	c3	-0.363
20	c3	-0.620
21	hc	0.185
22	hc	0.185
23	c3	0.079
24	c3	-0.056
25	hc	0.031
26	hc	0.031
27	c3	-0.152
28	c3	-0.075
29	hc	0.022
30	hc	0.022
31	c3	-0.048
32	hc	0.085
33	c3	-0.218
34	hc	0.060
35	hc	0.060
36	hc	0.060
37	cd	-0.092
38	cd	0.331
39	h4	0.138
40	h5	0.096
41	cd	-0.253
42	h4	0.190
43	cd	0.250
44	h5	0.113
45	cd	-0.177
46	h4	0.170
47	cd	0.358

48	h5	0.088
49	cd	-0.233
50	h4	0.194
51	cd	0.329
52	h5	0.089
53	cc	0.383
54	cc	0.382
55	cc	0.406
56	cc	0.249
57	na	-0.444
58	nc	-0.658
59	na	-0.452
60	nc	-0.598
61	na	-0.410
62	nc	-0.674
63	na	-0.499
64	nc	-0.642
65	c3	-0.075
66	hc	0.022
67	hc	0.022
68	c3	-0.152
69	c3	-0.056
70	hc	0.031
71	hc	0.031
72	c3	0.079
73	hc	0.066
74	c3	-0.620
75	hc	0.185
76	hc	0.185
77	c3	-0.363
78	c3	0.035
79	hc	0.043
80	hc	0.043
81	c3	-0.036
82	hc	0.106
83	c3	-0.353
84	hc	0.074
85	hc	0.074
86	c3	0.021
87	c3	-0.007
88	hc	0.014
89	hc	0.014
90	c3	0.104
91	c3	-0.379
92	hc	0.099
93	hc	0.099
94	cd	-0.233
95	cd	0.329
96	h4	0.194
97	h5	0.089
98	cd	-0.177

99	h4	0.170
100	cd	0.358
101	h5	0.088
102	cd	-0.253
103	h4	0.190
104	cd	0.250
105	h5	0.113
106	cc	0.406
107	cc	0.382
108	cc	0.383
109	nc	-0.642
110	na	-0.444
111	nc	-0.674
112	na	-0.499
113	nc	-0.598
114	na	-0.410
115	hn	0.363
116	hn	0.367
117	hn	0.369
118	hn	0.367
119	hn	0.376
120	hn	0.363
121	cd	-0.264
122	h4	0.207
123	cd	0.231
124	h5	0.111
125	cd	-0.166
126	h4	0.164
127	cd	0.187
128	h5	0.122
129	cd	-0.253
130	cd	0.298
131	h4	0.207
132	h5	0.097
133	c2	-0.118
134	c2	0.073
135	h4	0.182
136	h5	0.216
137	cd	-0.253
138	cd	0.298
139	h4	0.207
140	h5	0.097
141	cd	-0.166
142	cd	0.187
143	h4	0.164
144	h5	0.122
145	cd	-0.264
146	cd	0.231
147	h4	0.207
148	h5	0.111
149	cc	0.351

150	cc	0.421
151	cc	0.329
152	c2	0.119
153	cc	0.329
154	cc	0.421
155	cc	0.351
156	nc	-0.533
157	na	-0.425
158	nc	-0.546
159	na	-0.379
160	nc	-0.640
161	na	-0.397
162	na	-0.208
163	na	-0.299
164	nc	-0.640
165	na	-0.397
166	nc	-0.533
167	na	-0.425
168	nc	-0.546
169	na	-0.379
170	hn	0.355
171	hn	0.372
172	hn	0.352
173	hn	0.382
174	hn	0.352
175	hn	0.372
176	hn	0.355
177	hc	0.078
178	hc	0.066
179	hc	0.225
180	hc	0.045
181	hc	0.081
182	c3	-0.048
183	hc	0.085
184	c3	-0.218
185	hc	0.060
186	hc	0.060
187	hc	0.060
188	hc	0.045
189	hc	0.225
190	hc	0.078
191	hn	0.324
192	hn	0.376
193	hc	0.067
194	cd	-0.092
195	cd	0.331
196	h4	0.138
197	h5	0.096
198	cc	0.249
199	nc	-0.658
200	na	-0.452

201	hn	0.369

Table S3. Equilibrium bending parameters for the angles c2-na-hn and c2-c2-na

angle	$\theta_{ijk,0}$(deg)	
	original	modified
c2-na-hn	119.28	126.35
c2-c2-na	121.38	106.91

Table S4. NBO and RESP charges computed along the frustated rotation of the protonated central imidazole in the 15mer^{+}

		NBO			*RESP*	
φ	*-30*	*0*	*30*	*-30*	*0*	*30*
H_3[b]	0.488	0.487	0.491	0.324	0.315	0.327
N_3[b]	-0.542	-0.516	-0.536	-0.208	-0.245	-0.220
N_3[a]	-0.614	-0.601	-0.617	-0.658	-0.620	-0.667

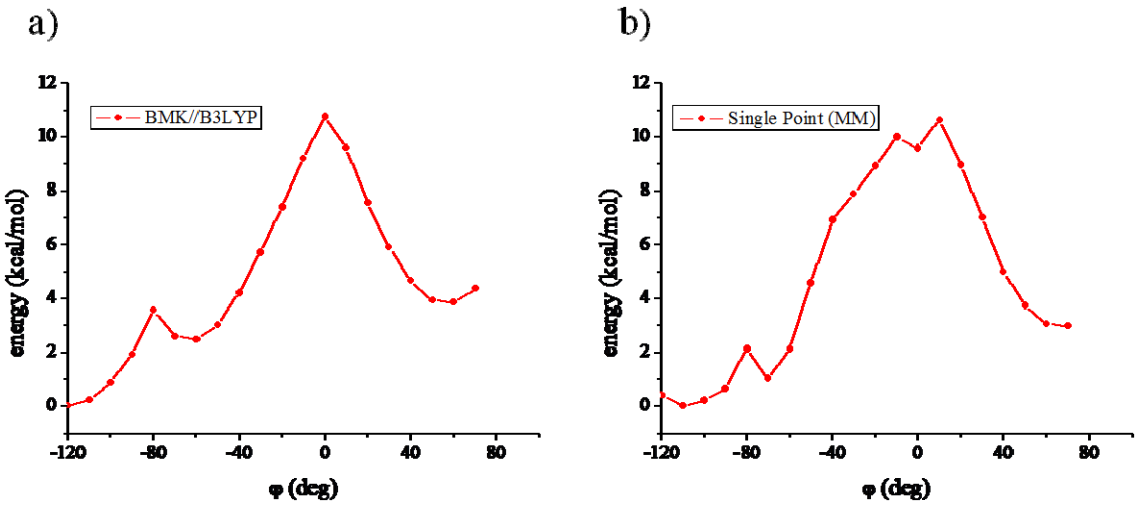

Figure S1. DFT (left) and MM (right) potential energy profile for the torsion around the dihedral angle φ. MM values have been obtained with the modified GAFF.

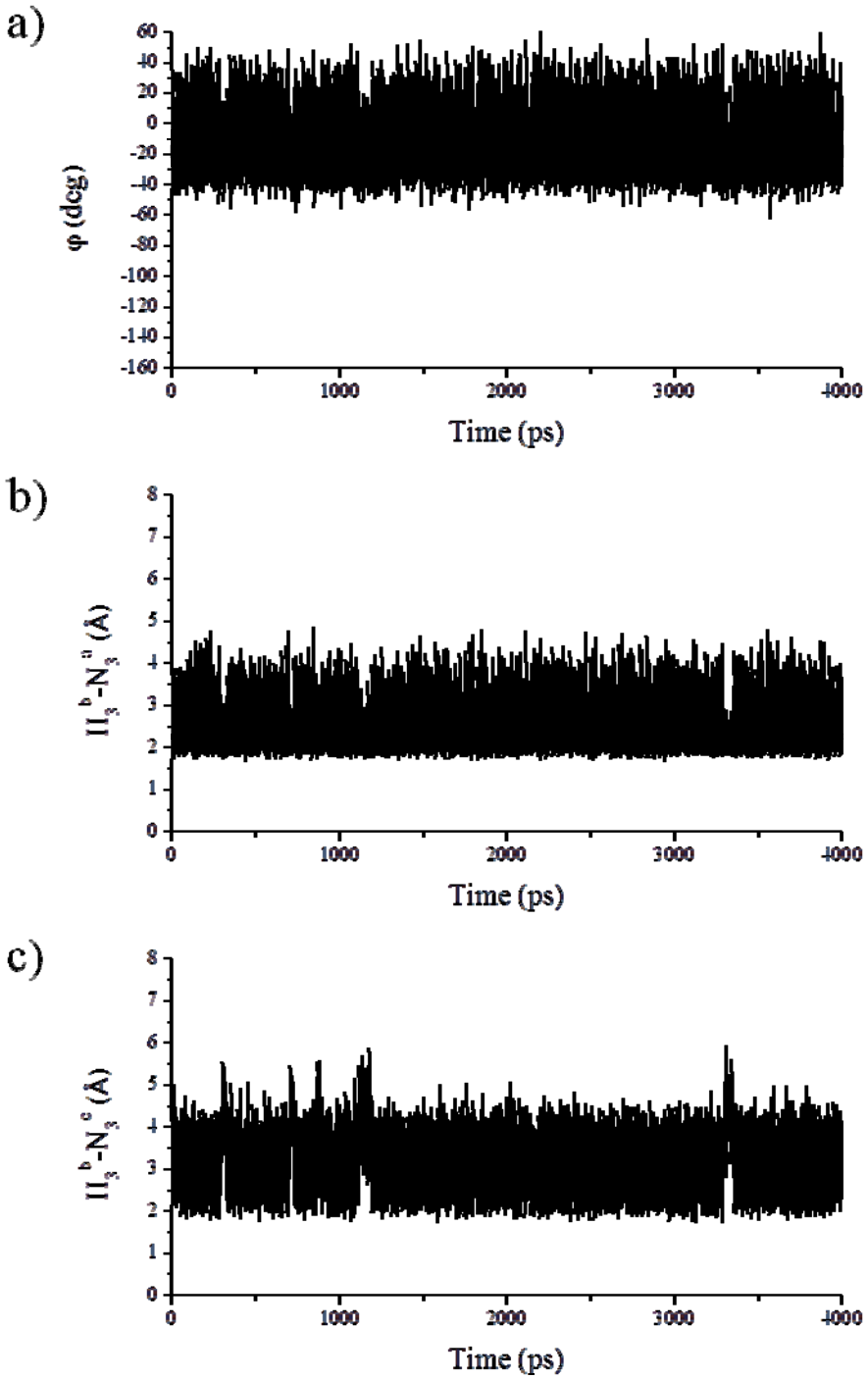

Figure S2. Variation of the dihedral φ (up), H_3^b-N_3^a distance (middle) and H_3^b-N_3^c distance (down) along the whole trajectory of 4 ns obtained for *15mer*$^+$.

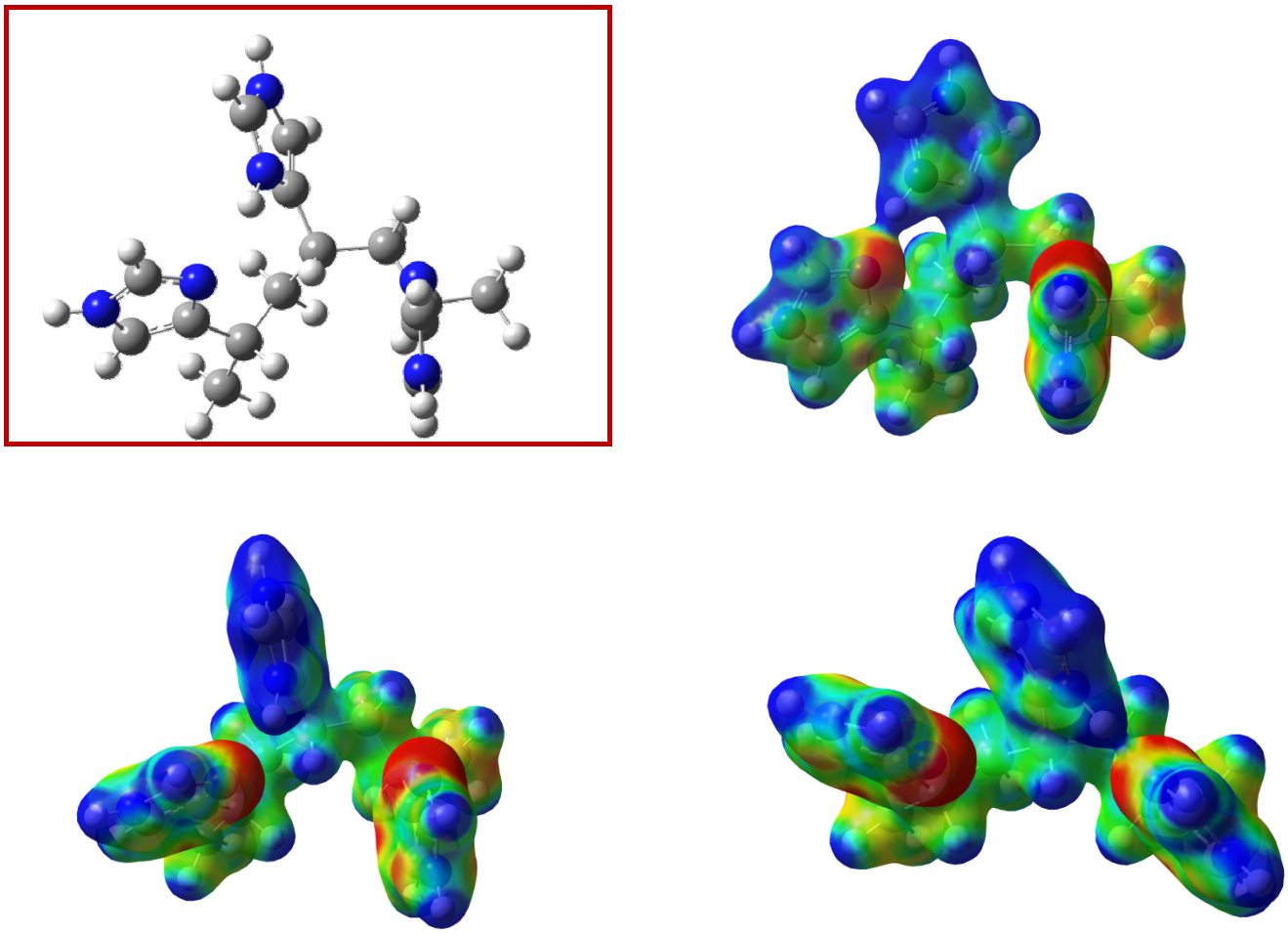

Figure S3. Electrostatic potential computed along the frustrated rotation of the φ ($H_{(5)}$-$C_{(4)}$-$C_{(19)}$-$N_{(21)}$):upper right φ=-30°, lower left φ=0°, lower right φ=30°

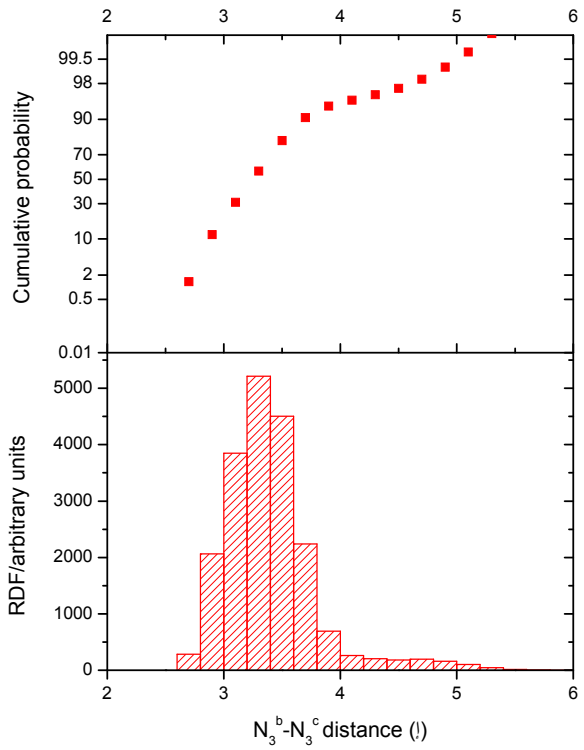

Figure S4. Occurrence of the N_3^b-N_3^c distance during the 4ns simulation.